Available online at www.sciencedirect.com
ScienceDirect
Journal of Power Sources 174 (2007) 805–809
JOURNAL OF POWER SOURCES
www.elsevier.com/locate/jpowsour

Short communication

Sb/O nano-composites produced via Spark Discharge Generation for Li-ion battery anodes

L. Simonin *, U. Lafont, N. Tabrizi, A. Schmidt-Ott, E.M. Kelder

TUDelft NanoStructured Matrials DelftChemTech, Julianalaan 136, 2628 BL Delft, The Netherlands

Available online 30 June 2007

Abstract

Spark Discharge Generation (SDG) was used to produce powders of 10–20 nm of Sb and antimony oxides. Different composite materials with different textures were obtained either with an amorphous passive layer of antimony oxide or with crystalline cubic Sb_2O_3. The composition and shape of the different mixtures, depending on the production and collection conditions, were analysed via XRD and HRTEM coupled with EDX. The effect of the nature and the content of the oxides on the electrode performances were studied using Swagelok cells, cycled galvanostatically with a MACCOR cycler.

Keywords: Spark Discharge Generation; Li-ion battery; Nanomaterials; Antimony; Antimony oxide

1. Introduction

Recently there has been a revived interest in using metals, alloys and intermetallics as anode materials for Li-ion batteries. The attraction for the use of these compounds is mainly due to their large capacity (higher than the one of carbonaceous materials). However, one of their main drawbacks is the fact that alloying reactions are non-topotactic. This induces many changes in the lattice and drastic volume changes upon charge and discharge. This circumstance results in a quick fading of the capacity. Antimony is known to form Li_3Sb [1–3] during the first discharge, which corresponds to a capacity of 660 mAh g^{-1}. This value is almost twice the theoretical capacity of graphite. The volume expansion leads to a rapid loss of capacity after a few cycles. In order to avoid or limit the volume expansion, two solutions are possible: the use of nano-particles and the use of a multi-phase material in which the active metal is buffered by a matrix or a layer of inactive material, e.g.: Sn within a matrix of Cu [4] or Sn within tin oxide forming a Li_2O matrix after the first cycle [5]. A very interesting technique to produce fine particles of any conductive material is called Spark Discharge Generation. It is possible to produce primary particles smaller than 20 nm. Schwyn et al. generated gold particles between 0.5 nm and 2 nm [6]. All these particles were produced with a non-negligible amount of oxide either as a layer or a matrix, which might play a buffering role.

2. Experiments

The synthesis was carried out via Spark Discharge Generation. This technique, which is schematised in Fig. 1 relies on the atomisation of electrodes by spark discharge. Two opposing cylindrical electrodes are mounted at adjustable distance. One electrode is connected to a high-voltage supply (TECHNIX CCR-15-p-750) in parallel with a variable capacitance and the other one is connected to the ground. The capacitor formed by the two electrodes and the carrier gas is periodically charged to its breakdown voltage. A spark is produced, in which a very high temperature (between 6000 K and 40,000 K [7]) is reached, inducing evaporation of the electrode material for a few nanoseconds. Then, a rapid cooling occurs leading to the formation of nanosized particles. A constant flow rate of inert gas is maintained in order to carry the particles away and to keep the breakdown voltage constant [8]. Antimony rods of 6 mm diameter from Goodfellow were used as electrodes. The electrode gap was 1 mm, the capacitance of the parallel capacitors was 20 nF, the carrier gas was either N_2 or Ar and the flow rate was 1.19 L min^{-1}. The operating conditions are described in detail in Table 1. Four different samples were produced, changing the carrier gas, the oxygen content of the reactor (with or without

* Corresponding author. Tel.: +31 15 278 5536.
E-mail address: l.simonin@tudelft.nl (L. Simonin).

0378-7753/$ – see front matter © 2007 Elsevier B.V. All rights reserved.
doi:10.1016/j.jpowsour.2007.06.197

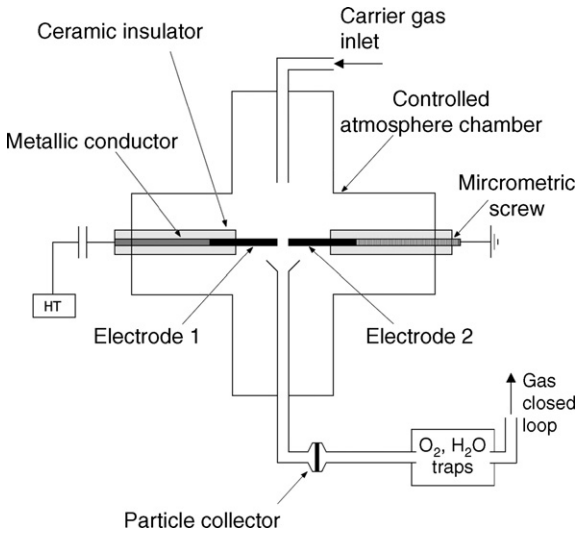

Fig. 1. Spark Discharge Generator.

oxygen and moisture traps) and the way to collect the powders (slow or fast exposure to air). Two commercial powders of Sb and Sb_2O_3 were also used as reference samples. One was an Alfa-Aesar micrometer-sized Sb powder, while the other one was Aldrich Sb_2O_3.

The samples were analysed by X-ray diffraction using a "Bruker Diffractplus" diffractometer operated with a copper Kα radiation of 1.54184 Å. Angular scans were carried out at a rate of 0.16° min^{-1} from $2\theta = 20°$ to 60°. Transmission electron microscopy (TEM) was performed using a Philips CM30T electron microscope with a LaB_6 filament as source of electrons and operated at 300 kV. Samples were mounted on Quantifoil® microgrids carbon polymer supported by a copper grid, placing a few droplets of a suspension of ground sample in ethanol on the grid, followed by drying at ambient conditions. The powder was then tested electrochemically in Swagelok-type cells with a Maccor (S-4000) battery cycler. A mixture of 80 wt% of active material and 20 wt% of carbon black from Alfa-Aesar was made in an agate mortar. The powder was placed directly on the bottom of the Swagelok cell. A galvanostatic test was performed at a constant gravimetric current density of 110 mA g^{-1}, between 0.5 V and 1.5 V. The carbon black was initially tested alone and showed a negligible effect on the overall capacity (less than 6% for the first discharge and less than 1% for the first charge and the subsequent cycles).

Table 1
Operating conditions (in bold: parameters that were changed)

	Sample			
	A	B	C	D
Breakdown voltage (kV)	0.5	0.5	2	0.5
Capacitance (nF)	20	20	20	20
Carrier gas	Ar	Ar	**N_2**	Ar
Gas flow rate (L min^{-1})	1.19	1.19	1.19	1.19
Electrodes gap (mm)	1	1	1	1
Oxygen trap	Yes	Yes	**No**	Yes
Exposure to air	Slow	Slow	Slow	Fast

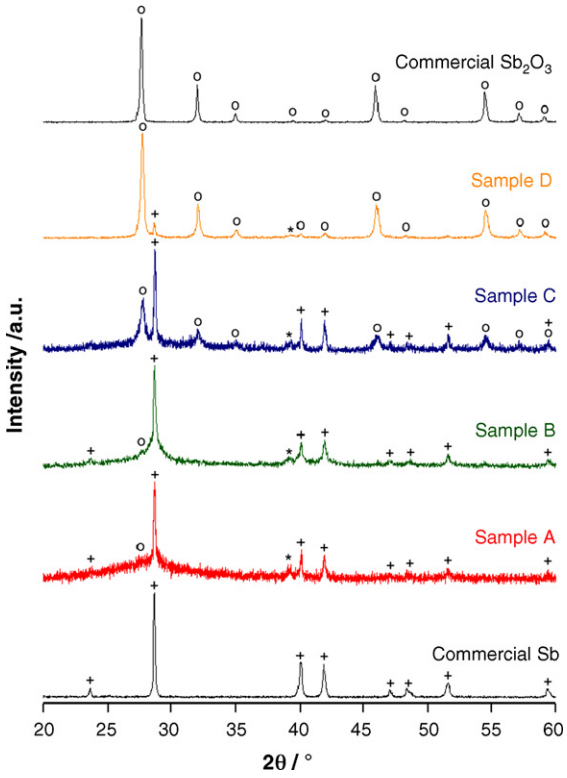

Fig. 2. X-ray diffractograms of the different commercial reference powders and SDG samples. (◯) Sb_2O_3; (+) Sb; (*) impurity.

3. Results and discussion

XRD patterns (Fig. 2) of the different powders produced show crystalline particles of antimony with broader peaks than those of the commercial powder. The patterns of samples C and D show peaks due to cubic Sb_2O_3. This can be explained by the presence of a significant amount of oxygen during the production of sample C or right after the production for sample D due to a fast exposure to air. Moreover nano-powders of Sb are strongly pyrophoretic. This means that even oxygen traces present in the reaction chamber or in the storage boxes are readily taken up by the Sb. In sample D, oxygen can be taken up during exposure in air before further sampling. In the case of samples A and B, a much smaller peak (at 28°) shows the presence of traces of Sb_2O_3. This can be explained by the fact that the sample is very slowly exposed to air, which leads to the formation of a thin passive layer of amorphous oxide. However, sample A shows a greater amorphous background than sample B.

From the TEM pictures (Fig. 3), sample A shows a bulk of amorphous antimony oxide with very small particles (below 10 nm) of Sb dispersed in it. Sample B is a porous network of antimony crystalline particles with no evidence of an amorphous compact matrix like in sample A. Sample C shows more or less the same structure as sample B. In sample D "square"-shaped particle are present in contrast to samples B and C. These particles are most likely attributed to a Sb_2O_3 phase.

The energy-dispersive spectra (EDS) displayed in Fig. 4 show a significant amount of oxygen in all the samples which were investigated. EDS was not performed for sample A, but the

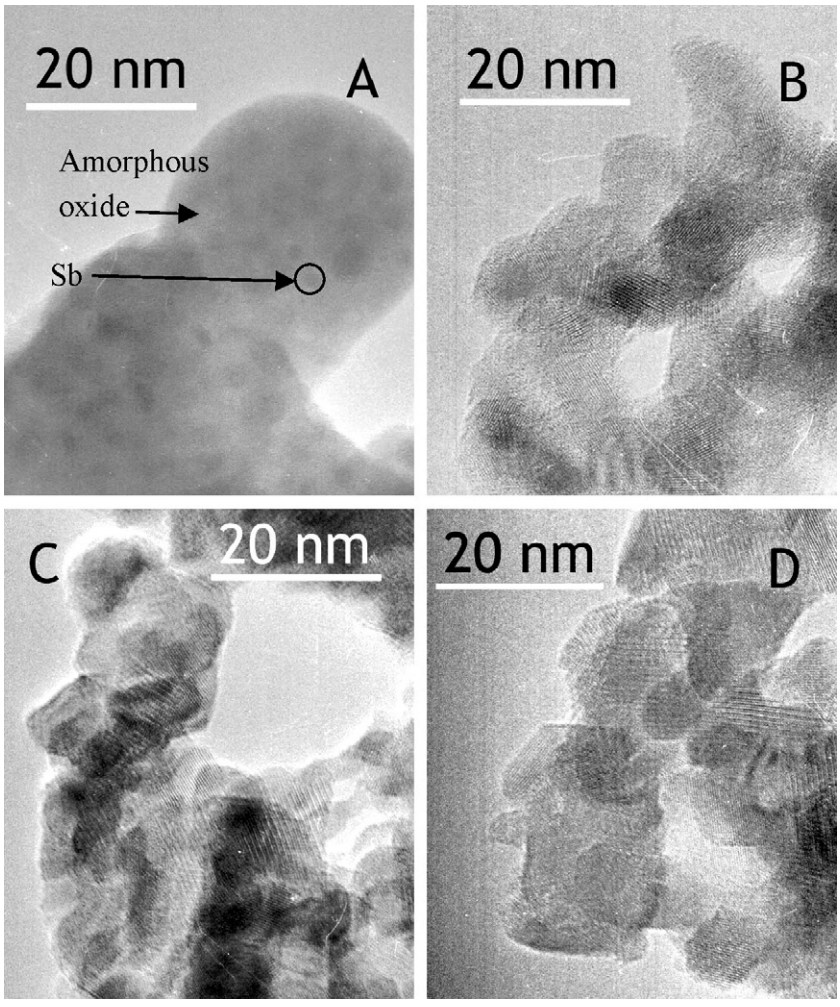

Fig. 3. Transmission electron microscopy of sample A (top left), sample B (top right), sample C (bottom left) and sample D (bottom right).

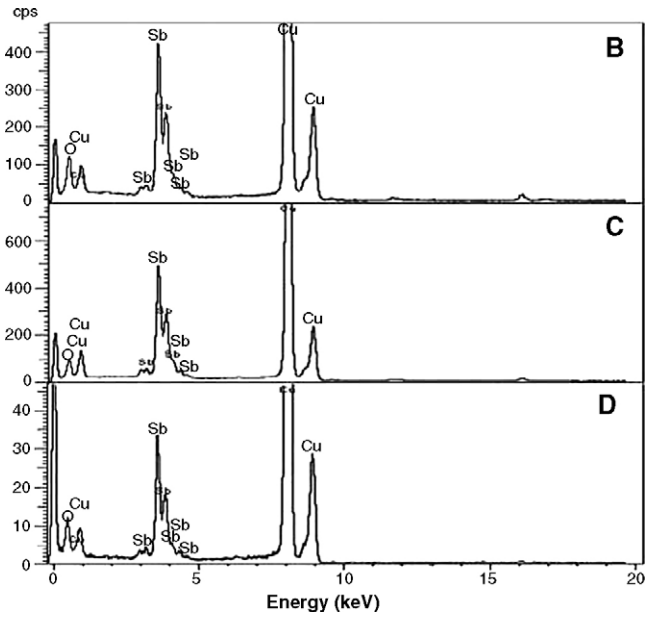

Fig. 4. Energy-dispersive spectroscopy of samples B–D.

presence of oxides is suggested by galvanostatic measurements (see Fig. 5).

Fig. 5 represents the first cycle of the galvanostatic tests. The discharge curve of the commercial Sb powder shows, after a sharp voltage drop, a clear plateau around 0.8 V. This plateau reveals a capacity of 630 mAh g^{-1}, equal to $Li_{2.86}Sb$. During the charge, the curve shows a similar feature but at higher voltage due to significant polarisation. The capacity that can be reversibly cycled then becomes 530 mAh g^{-1}.

The capacity that can be reversibly cycled then becomes 530 mAh g^{-1}. The discharge curve of Sb_2O_3 can be separated in two main plateaus. The lower voltage part (1.1 V down to 0.5 V) is due to Li uptake in metallic Sb, which has been formed by the reduction of Sb_2O_3 in the first part of the discharge, i.e. occurring at 1.4 V. The reduction capacity of Sb_2O_3 is about 300 mAh g^{-1}.

When looking at the charge–discharge curves of the samples synthesised via SDG, sample D reveals a similar behaviour, and therefore, we may infer that this sample contains a significant amount of oxide, which is crystalline. These results are concordant with the XRD measurements and the EDS analysis, showing mainly antimony oxide. However, the whole curve is 0.1 V below that of the commercial one, which can be explained

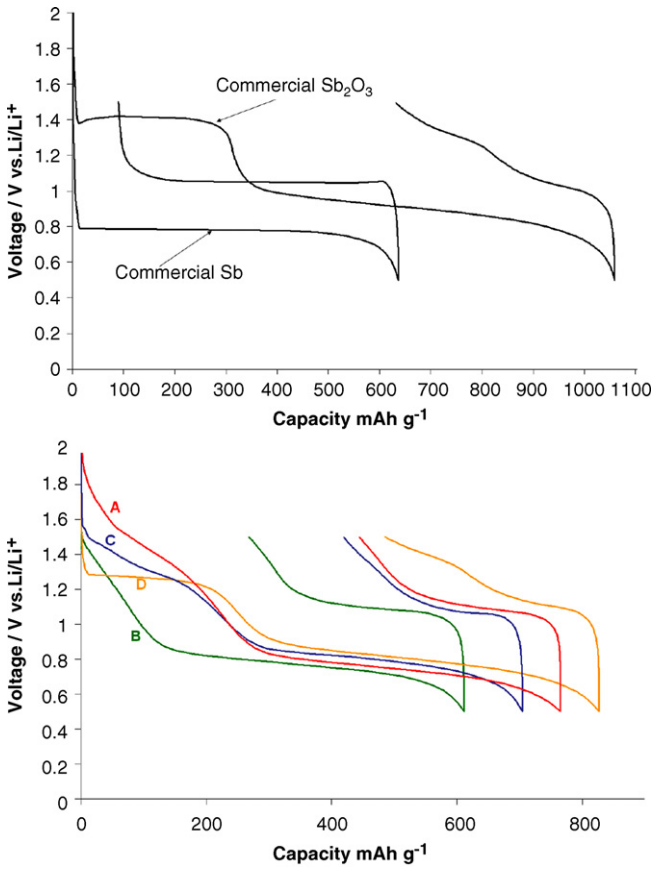

Fig. 5. First cycle of galvanostatic tests for samples A–D (bottom graph) and commercial powders (top graph).

by a higher cell resistance due to completely different texture and size of particles. Since all the other samples also contain oxygen, a plateau may be expected for these samples too. Indeed this is the case, however it is striking that the curves during reduction of the oxide show a sloping shape feature. This indicates an insertion that may be described via the formation of a solid solution, which is most likely here an amorphous phase.

The reactions taking place during discharge of Sb_2O_3 and Sb are, respectively described in Eqs. (1) and (2) [1–3,8,9],

$$12Li + Sb_2O_3 \rightarrow 3Li_2O + 2Li_3Sb \quad (1)$$

$$3Li + Sb \rightarrow Li_3Sb \quad (2)$$

Regarding the normalised capacity curves (Fig. 6), the ratio between the total capacity and the capacity of the first region ("oxide plateau") is 30%/70% for samples A, C and D and only differs in the case of sample B (around 20%/80%). Sample B is the only one that neither contains a big amount of crystalline Sb_2O_3 (as it is revealed for samples C and D by XRD) nor a bulk amorphous oxide matrix (as established for sample A by TEM). Taking into account that the first plateau/slope is only due to reduction of oxide into Li_2O and Sb, the difference in the ratios can now be explained by at least two different mechanisms. The simplest one is that the samples A, C and D contain Sb_2O_3 only. However, this is not in line with the TEM and XRD observations. The other explanation can be that Sb_2O_3 and its products during the reduction (Li_3Sb and L_2O (Eq. (1))), prevent Li ions to enter the Sb already present at the beginning.

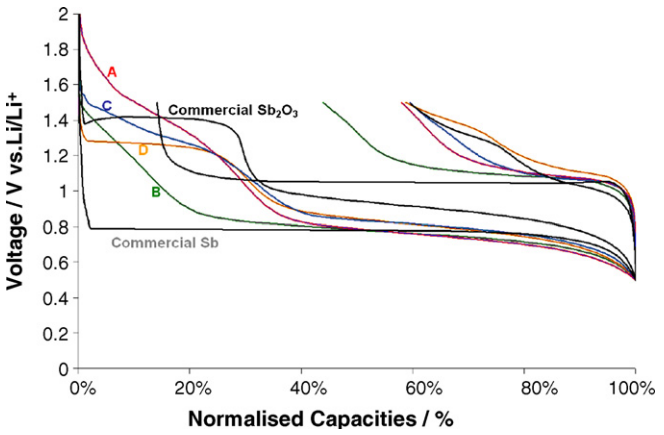

Fig. 6. Normalised capacity curves for the first cycle of samples A–D and commercial Sb and Sb_2O_3.

4. Conclusion

Antimony–antimony oxide nanostructured materials were successfully produced with different textures, compositions, and crystallinities, depending on the different experimental parameters. Production of pure antimony particles still seems to be very challenging: it appears very difficult to get rid of an amorphous oxide surface layer, which represents a significant fraction of the volume regarding the size of the particles. In that respect, reducing the size of the metallic particles automatically increases the presence of irreversible oxides and impurities. The electrochemical behaviour of each material leads to the conclusion that their texture is probably a very important factor for good insertion in both Sb and antimony oxide particles. The cycling behaviour was not reported in the present work because, at this moment, it is still unclear whether the presence of the oxide matrix leads to an effective stabilisation of cycleability. But it is clear that this matrix has to be porous enough to allow lithium to interact with Sb particles.

Acknowledgements

The authors want to thank the ALISTORE European Network of Excellence for financial support, and sharing of knowledge and equipment.

We also want to express our gratitude to Prof. Joop Schoonman, Dan Simon and Frans Ooms for their scientific and technical assistance.

References

[1] L. Aldon, A. Garcia, J. Olivier-Fourcade, J.-C. Jumas, F.J. Fernandez-Madrigal, P. Lavela, C. Perez Vicente, J.L. Tirado, J. Power Sources 119–121 (2003) 585.

[2] L.M.L. Fransson, J.T. Vaughey, R. Benedek, K. Edström, J.O. Thomas, M.M. Thackeray, J. Power Sources 119–121 (2003) 64.

[3] A.J. Kropf, H. Tostmann, C.S. Johnson, J.T. Vaughey, M.M. Thackeray, Electrochem. Commun. 3 (2001) 244.
[4] K.D. Kepler, J.T. Vaughey, M.M. Thackeray, J. Power Sources 81/82 (1999) 383.
[5] N. Pereira, L.C. Klein, G.G. Amatucci, Solid State Ionics 167 (2004) 29.
[6] C. Helsper, W. Molter, F. Loffler, C. Wadenpohl, S. Kaufmann, G. Wenninger, Atmos. Environ. A 27 (1993) 1271.
[7] C.M. Cundall, J.D. Craggs, Spectrochim. Acta 9 (1957) 68.
[8] S. Schwyn, E. Garwin, A. Schmidt-Ott, J. Aerosol Sci. 19 (1988) 639.
[9] H. Li, X. Huang, L. Chen, Solid State Ionics 123 (1999) 189.